

High-Resolution X-Ray Lensless Imaging by Differential Holographic Encoding

Diling Zhu,^{1,2,*} Manuel Guizar-Sicairos,³ Benny Wu,^{1,2} Andreas Scherz,² Yves Acremann,^{4,†} Tolek Tyliczszak,⁵ Peter Fischer,⁶ Nina Friedenberger,⁷ Katharina Ollefs,⁷ Michael Farle,⁷ James R. Fienup,³ and Joachim Stöhr⁸

¹*Department of Applied Physics, Stanford University, Stanford, California, USA*

²*Stanford Institute for Material and Energy Science, SLAC National Accelerator Laboratory, Menlo Park, California, USA*

³*The Institute of Optics, University of Rochester, Rochester, New York, USA*

⁴*PULSE Center for Energy Science, SLAC National Accelerator Laboratory, Menlo Park, California, USA*

⁵*Chemical Sciences Division, Advanced Light Source, Lawrence Berkeley National Laboratory, Berkeley, California, USA*

⁶*Center for X-ray Optics, Lawrence Berkeley National Laboratory, Berkeley, California, USA*

⁷*Department of Physics and Center for Nanointegration Duisburg-Essen (CeNIDE), Universität Duisburg-Essen, Duisburg, Germany*

⁸*Linac Coherent Light Source, SLAC National Accelerator Laboratory, Menlo Park, California, USA*

(Received 25 February 2010; revised manuscript received 23 June 2010; published 20 July 2010)

We demonstrate in the soft x-ray regime a novel technique for high-resolution lensless imaging based on differential holographic encoding. We have achieved superior resolution over x-ray Fourier transform holography while maintaining the signal-to-noise ratio and algorithmic simplicity. We obtain a resolution of 16 nm by synthesizing images in the Fourier domain from a single diffraction pattern, which allows resolution improvement beyond the reference fabrication limit. Direct comparisons with iterative phase retrieval and images from state-of-the-art zone-plate microscopes are presented.

DOI: [10.1103/PhysRevLett.105.043901](https://doi.org/10.1103/PhysRevLett.105.043901)

PACS numbers: 42.40.Kw, 61.05.cf, 68.37.Yz

X-ray free electron lasers (X-FELs) will soon offer femtosecond pulses of laterally coherent x-rays with sufficient intensity to record single-shot coherent scattering patterns for nanoscale imaging [1–4]. Pump-probe [3] and split-delay [5,6] techniques will bring sequential snapshots, even movies, that can help deepen our understanding of a plethora of transient physical and chemical processes at nanometer length and femtosecond time scales, e.g., fluctuation in nonequilibrium systems, external field driven energy and angular momentum transfer processes, and ultrafast structural changes. A key to ultrafast motion pictures is fast and reliable inversion of the recorded coherent scattering intensity patterns. In this Letter, we demonstrate, in the soft x-ray regime, a novel noniterative lensless imaging technique based on differential holographic encoding, previously suggested by Guizar-Sicairos and Fienup [7,8], termed holography with extended reference by autocorrelation linear differential operation (HERALDO). We found that the technique not only provides instant high-resolution reconstruction, but also proves to be robust against data imperfections. In particular it reduces artifacts arising from the commonly-missing central low q data. By Fourier domain synthesis we were able to achieve a resolution beyond the limit of reference fabrication processes. Our method compares favorably with other state-of-the-art imaging techniques, as we provide direct comparison with images obtained by Fourier transform holography FTH [9,10], iterative phase retrieval image reconstruction algorithm [11], and zone-plate microscopy techniques [12–14].

HERALDO is an off-axis holographic technique in which the reference wave emerges from a sharp feature or edge on an extended structure, and the image is differ-

entially encoded in the Fourier transform of the coherent scattering intensity pattern [7,15]. Unlike previous x-ray lensless holography experiments [10,16], where resolution was determined by the width of small reference features, the resolution of HERALDO is instead given by the extent of the derivative of the edge response, as illustrated in Figs. 1(a) and 1(b). The differential operation on the autocorrelation can be realized by the multiplication of the hologram intensity with an equivalent Fourier domain filter [7,8], followed by an inverse Fourier transform. As can be seen in Fig. 1(e), the Fourier domain decoding filter for HERALDO is typically a high pass filter; i.e., the information about the object is preferentially encoded in the high q part of the coherent scattering intensity. This renders the method less influenced by the loss of the central part of the data, due to the overlap with the direct beam or the beam stop shadow, which can become an obstacle to achieving high quality reconstructions for previous methods.

In the first experiment, using a high contrast “Swiss cheese” pattern as the object, shown in Fig. 2, we demonstrate that HERALDO can deliver sharper images than FTH, without compromising the signal-to-noise ratio (SNR). The object and the references were fabricated with a focused ion beam (FIB) on a 200 nm thick gold film supported by a 100 nm thick silicon nitride window. The reference structures chosen in this case were an “L” shaped slit and a small pinhole for comparison with FTH. Because the size of the reference pinhole fabricated with FIB is highly sensitive to the milling conditions, a series of samples, identical except with varying ion-beam doses for the references, were fabricated. We chose the sample that had the smallest reference pinhole (~ 40 nm) among the

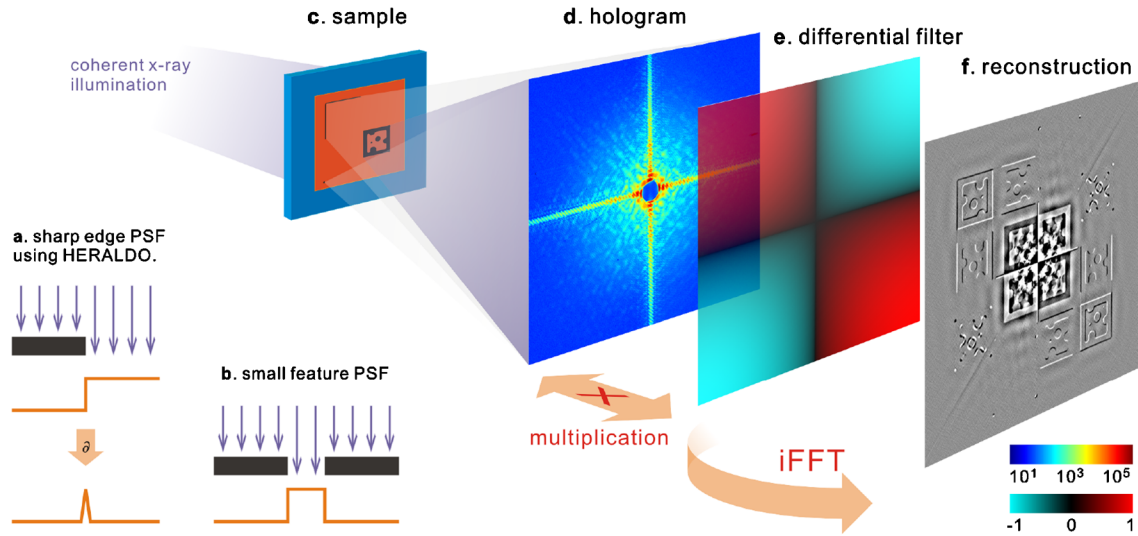


FIG. 1 (color online). HERALDO schematics. (a) and (b) illustration comparing the point spread function (PSF) from a sharp edge after differential operation and the PSF from a small feature, e.g., a reference hole. (c) The object and reference structures are illuminated with a coherent x-ray beam. (d) The incident beam is scattered by both the object and the references, and a hologram is recorded by a 2D array detector in the far field; intensity shown here in log scale. (e) The diffraction intensity is multiplied by a linear differential filter. (f) A single Fourier transform delivers three relief images of the object from which the final reconstruction is computed.

series. On the other hand, the width of the “L”-shaped slit (~ 20 nm) appears to be not as sensitive to the variation in ion-beam exposure time, which greatly simplifies the HERALDO reference fabrication. The slit width determines the resolution in the direction perpendicular to the slit and edge sharpness determines the resolution along the slit.

X-ray coherent scattering data were recorded at BL13-3 at the Stanford Synchrotron Radiation Lightsource (SSRL), with x-ray energy of 650 eV (1.9 nm). The detector (1340×1300 pixels, pixel size $20 \mu\text{m}$) was placed 240 mm from the sample. A ~ 1.1 mm diameter beam stop was used to block the central region of approximately 60 pixels in diameter. Reconstructions can be obtained from each end of the L-shaped slit individually by applying a single directional derivative (first order differential operator) along either arm of the L. This yields two reconstructions with higher resolution than FTH but with reduced SNR due to the narrower slits being weaker references. We found it to be more robust to apply a second order decoding filter as in Fig. 1(e), which also provides a much stronger suppression of the artifacts due to the beam stop, to obtain three different directional derivatives of the object as shown in Fig. 2(c) [17]. These are equivalent to relief images having illumination from different angles. The problem is then reduced to finding an object that can reproduce all three derivatives, a well-studied problem for wave front reconstruction from Shack-Hartmann measurements [18–20]. For reconstruction we generalized the technique for phase reconstruction for digital shearing laser interferometry in [21] to complex-valued objects. This leads to a robust reconstruction that achieves the same level of SNR as FTH with improved resolution. The results

are shown in Fig. 2(d), compared with the FTH reconstruction shown in Fig. 2(b).

The resolution of HERALDO can be further extended beyond the reference fabrication limit by combining images obtained from independent sharp features on a single extended reference through a noniterative computation. We demonstrated this capability by imaging Fe nanocubes [22] using a triangular reference, as shown in Fig. 3(a). The sample contained nanocubes 18 nm in size dispersed on a silicon nitride membrane with $\sim 50\%$ coverage. The other side of the nitride membrane was coated with a $1 \mu\text{m}$ thick gold film. A $900 \text{ nm} \times 900 \text{ nm}$ square aperture defined the viewing window. The reference triangle was milled through the sample. A hologram was recorded on the iron L_3 resonance [708 eV, or 1.76 nm, see Fig. 3(b)] with the sample-detector distance of 150 mm. Total exposure time was 20 minutes. Three reconstructions can be calculated instantly from each individual corner, as shown in Fig. 3(c).

The corners of the triangle in reality always have a finite curvature determined by the FIB radius. They scatter photons preferentially along different directions, sampling the frequency spectrum of the object with high SNR in complementary regions. We therefore expect the images reconstructed from each corner to have higher resolution along different directions. A composite image of higher overall resolution can be obtained by combining the three images using a multiframe Yaroslavsky-Caulfield filter [23], a summation in Fourier space that is weighted by the frequency-dependent SNR of the images. We use this filter for noise regularization only, since a good estimate of the point spread functions (necessary for deconvolution) is not available. The combined result shows a significant

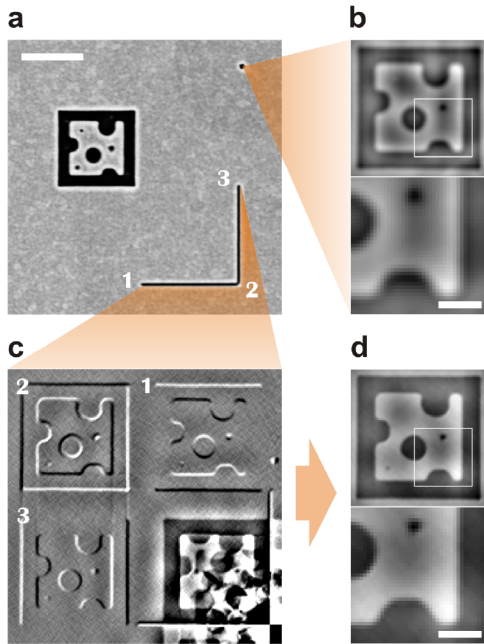


FIG. 2 (color online). “Cheese” sample reconstructions. (a) SEM overview ($1\ \mu\text{m}$ scale bar). (b) FTH reconstruction and the magnified view of the lower right corner ($200\ \text{nm}$ scale bar). (c) The three relief images obtained. (d) HERALDO reconstruction from (c) and the magnified view of the lower right corner ($200\ \text{nm}$ scale bar).

improvement of the reconstruction resolution beyond the reference fabrication limitation, resolving single-particle rows and gaps, as shown in Fig. 3(d). The resolution determined by line cuts at the edges of different nanocube clusters is $16\ \text{nm}$ or better, an example of which is shown in Fig. 4(f).

The HERALDO reconstruction provided a good support constraint for performing phase retrieval using an iterative transform algorithm (ITA) [11] on the same coherent scattering data. For the reconstruction, every 45 hybrid-input-output iterations followed by 5 iterations of error reduction [11] were repeated 20 times, for a total of 1000 iterations. We used an expanding weighting function on the measured data, as described in [24,25]. The algorithm was allowed to freely interpolate the data occluded by the beam stop and we used Fourier weighted projections [25] on the pixels with values less than zero after background subtraction. Ten reconstructions from random starting guesses were registered (subpixel translation [26] and defocus) and averaged for the final image shown in Fig. 4(c). The best focus position was set for optimal nanocube contrast. The resolution is determined by the line cut [Fig. 4(c) and 4(f)] and the 10%–90% criterion to be $24\ \text{nm}$. This resolution corresponds to the phase retrieval transfer function as defined in [27] cutoff at 60%. For this experiment, HERALDO achieved higher resolution while ITA was able to recover the low frequency information that was lost due to the beam stop. Notice that in the outer region of the measured diffraction pattern, where the high-resolution information

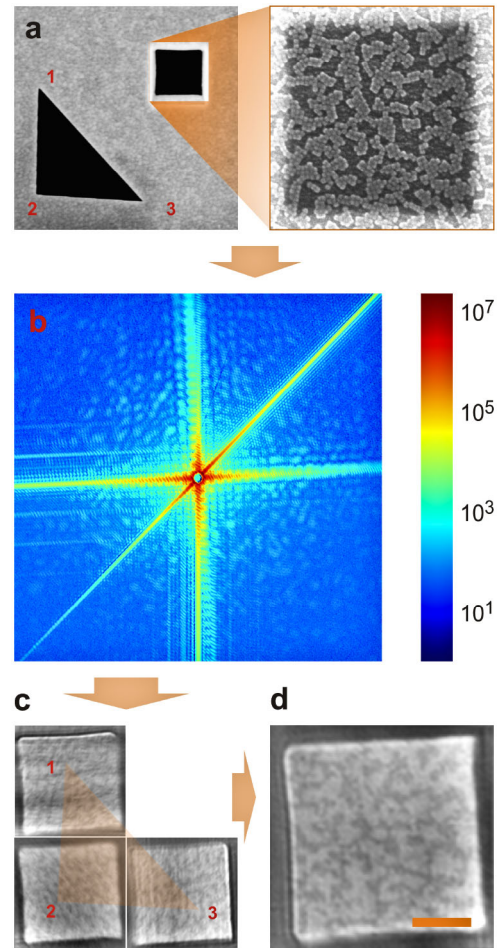


FIG. 3 (color online). Nanocube reconstruction. (a) SEM images of the sample: overview (left) and nanocubes within the square aperture supported by Si_3Ni_4 (right). (b) Recorded number of photons (central 650×650 pixels) in log scale. (c) Individual images obtained from the three corners are combined to obtain the final reconstruction in (d) ($300\ \text{nm}$ scale bar).

resides, the SNR can be too low for the phase to be consistently recovered by ITA. However, the fringe contrast remains distinguishable, which we believe allows the phase of the object field to be recovered deterministically by holography. There is evidence that, with longer exposure, ITA can improve on the holographic reconstruction resolution [28], while holography itself works surprisingly well with a small number of scattered photons [29].

We also compare the HERALDO results with the images obtained with state-of-the-art zone-plate based soft x-ray imaging instruments on the $\text{Fe}\ L_3$ resonance. Figure 4(d) is a scanning transmission x-ray microscope (STXM) [12] image obtained at the Advanced Light Source (ALS) BL 11.0.2 with a $20\ \text{nm}$ focusing zone plate. The scan used a $7\ \text{nm}$ step size and a total x-ray exposure time of 15 min. As expected, the STXM proves to be better at preserving the overall contrast. The image resolution in this case is limited by vibrations, and by stage and beam intensity drifts between each line scan, which can be seen from the diago-

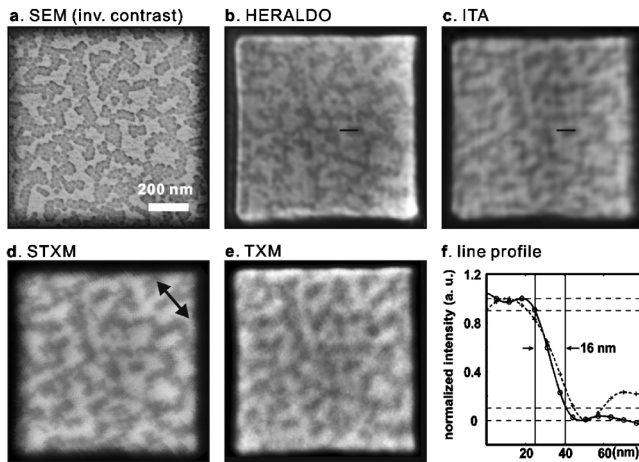


FIG. 4. Comparison of different methods. (a) SEM image with the contrast inverted for easier comparison. (b) HERALDO reconstruction, (c) ITA result. (d) STXM image; scanning direction indicated by arrow. (e) TXM image. (f) Comparison of line cut profiles as indicated in (b) for HERALDO (circles, solid line fitting) and (c) for ITA (crosses, dashed fitting). HERALDO reconstruction gives 16 nm resolution according to the 10%-90% criterion compared with 24 nm for ITA.

nal streaks. Figure 4(e) was obtained with the full field transmission x-ray microscope (TXM) XM1 at ALS BL 6.1.2 [13,14] using a 25 nm zone plate as the high-resolution objective lens. Five images of 1.2 s exposure were averaged for the final image. The higher noise level of the TXM image was a consequence of the shorter exposure time. In comparison, while zone-plate based methods represent a more general and versatile class of microscopy techniques, HERALDO clearly provides a single-shot compatible imaging platform that is capable of delivering superior resolution, and at the same time allows the study of nonrepeatable dynamic processes using the X-FEL.

In conclusion, we have demonstrated high-resolution holographic diffractive imaging using HERALDO at x-ray wavelengths. We find that the performance of this technique compares well with ITA and zone-plate imaging techniques. We identify HERALDO as a very promising approach for imaging at X-FEL sources because of its compatibility with single-shot imaging, its simplified reference fabrication, its fast and simple reconstruction algorithm, and its inherent robustness to the missing central part of the data. All parameters relevant to the Fourier decoding filter can be obtained directly from the data; thus no *a priori* quantitative knowledge of the object or reference is needed. A clever combination of reconstructions from individual sharp features can significantly increase the resolution, sensitivity, and SNR of the reconstructions. Using coded arrays of similar sharp features as HERALDO references can potentially further improve the imaging efficiency [16]. Our new concept offers a platform for element-specific single-shot nanoscale imaging of transient magnetic configurations and

correlations in ensembles of nanoparticles [30,31]. We envision the implementation of HERALDO to free space imaging of nanoparticles and clusters [32] by introducing heavy-element nanostructures with sharp edges into the particle beams. These known nanostructures could, in case of coincidental placement, serve as extended references.

The authors acknowledge support by the DOE, Office of Science, Basic Energy Sciences. Financial support by the DFG (SFB445) and the DAAD is also acknowledged. Fe nanocubes were synthesized by A. Shavel.

*Present address: Laboratorium f. Festkörperphysik, ETH Zürich, Zürich, Switzerland.

†Corresponding author.
dlzhu@stanford.edu

- [1] J. Miao, P. Charalambous, J. Kirz, and D. Sayre, *Nature (London)* **400**, 342 (1999).
- [2] H. N. Chapman *et al.*, *Nature Phys.* **2**, 839 (2006).
- [3] A. Barty *et al.*, *Nat. Photon.* **2**, 415 (2008).
- [4] A. Ravasio *et al.*, *Phys. Rev. Lett.* **103**, 028104 (2009).
- [5] R. Mitzner *et al.*, *Proc. SPIE Int. Soc. Opt. Eng.* **5920**, 59200D (2005).
- [6] W. Roseker *et al.*, *Opt. Lett.* **34**, 1768 (2009).
- [7] M. Guizar-Sicairos and J. R. Fienup, *Opt. Express* **15**, 17592 (2007).
- [8] M. Guizar-Sicairos and J. R. Fienup, *Opt. Lett.* **33**, 2668 (2008).
- [9] I. McNulty *et al.*, *Science* **256**, 1009 (1992).
- [10] S. Eisebitt *et al.*, *Nature (London)* **432**, 885 (2004).
- [11] J. R. Fienup, *Appl. Opt.* **21**, 2758 (1982).
- [12] A. L. D. Kilcoyne *et al.*, *J. Synchrotron Radiat.* **10**, 125 (2003).
- [13] W. Chao *et al.*, *Nature (London)* **435**, 1210 (2005).
- [14] W. Chao *et al.*, *Opt. Express* **17**, 17669 (2009).
- [15] S. G. Podorov *et al.*, *Opt. Express* **15**, 9954 (2007).
- [16] S. Marchesini *et al.*, *Nat. Photon.* **2**, 560 (2008).
- [17] M. Guizar-Sicairos *et al.*, *Opt. Lett.* **35**, 928 (2010).
- [18] D. L. Fried, *J. Opt. Soc. Am.* **67**, 370 (1977).
- [19] R. H. Hudgin, *J. Opt. Soc. Am.* **67**, 375 (1977).
- [20] W. H. Southwell, *J. Opt. Soc. Am.* **70**, 998 (1980).
- [21] S. T. Thurman and J. R. Fienup, *J. Opt. Soc. Am. A* **25**, 983 (2008).
- [22] A. Shavel *et al.*, *Adv. Funct. Mater.* **17**, 3870 (2007).
- [23] L. P. Yaroslavsky and H. J. Caulfield, *Appl. Opt.* **33**, 2157 (1994).
- [24] J. R. Fienup, *Opt. Express* **14**, 498 (2006).
- [25] M. Guizar-Sicairos and J. R. Fienup, *J. Opt. Soc. Am. A* **25**, 701 (2008).
- [26] M. Guizar-Sicairos and J. R. Fienup, *Opt. Lett.* **33**, 156 (2008).
- [27] H. N. Chapman *et al.*, *J. Opt. Soc. Am. A* **23**, 1179 (2006).
- [28] R. L. Sandberg *et al.*, *Opt. Lett.* **34**, 1618 (2009).
- [29] W. F. Schlotter *et al.*, *Appl. Phys. Lett.* **89**, 163112 (2006).
- [30] T. M. Hermans *et al.*, *Nature Nanotech.* **4**, 721 (2009).
- [31] V. Salgueirino-Maceira *et al.*, *J. Magn. Magn. Mater.* **303**, 163 (2006).
- [32] M. J. Bogan *et al.*, *Nano Lett.* **8**, 310 (2008).